Word count: 3060 words; 3 figures, 1 table

TOPOGRAPHY OF ACTIVATION DEFICITS IN SCHIZOPHRENIA DURING P300 TASK RELATED TO COGNITION AND STRUCTURAL CONNECTIVITY

Vicente Molina* [1,2,3,4], Alejandro Bachiller [5,6] , Rodrigo de Luis [2,8], Alba Lubeiro [1,2], Jesús Poza[4,6,7], Roberto Hornero[4,6,7], Joan Francesc Alonso [5,9], Miguel Angel Mañanas [5,9] Patricia Marqués [3], y Sergio Romero [5,9]

1- Psychiatry Department, School of Medicine, University of Valladolid, Av. Ramón y Cajal, 7, 47005 Valladolid, Spain.

2- Biomedical Research Institute of Salamanca (IBSAL)

3- Psychiatry Service, Clinical Hospital of Valladolid, Ramón y Cajal, 3, 47003 Valladolid, Spain.

4- Neurosciences Institute of Castilla y León (INCYL), Pintor Fernando Gallego, 1, 37007 University of Salamanca, Spain.

5- Automatic Control Department (ESAII), Biomedical Engineering Research Center (CREB), Polytechnic University of Catalonia, Barcelona, Spain

6- Biomedical Engineering Group, ETS Ingenieros de Telecomunicación, University of Paseo de Belén, 15, 47011, Valladolid, Spain

7- Instituto de Investigación en Matemática (IMUVA), University of Valladolid, Spain

8- Imaging Processing Laboratory, University of Valladolid, Paseo de Belén, 15, 47011 Valladolid, Spain.

9- CIBER-BBN, Biomedical Research Networking Center in Bioengineering, Biomaterials and Nanomedicine, Spain

* Corresponding author

Email: vicente.molina@uva.es

Tel: +34 983 423 200

ABSTRACT:

Background: The study of cerebral underpinnings of schizophrenia may benefit from the high temporal resolution of electromagnetic techniques, but its spatial resolution is low. However, source imaging approaches such as low-resolution brain electromagnetic tomography (LORETA) allow for an acceptable compromise between spatial and temporal resolutions.

Methods: We combined LORETA with 32 channels and 3-Tesla diffusion magnetic resonance (Dmr) to study cerebral dysfunction in 39 schizophrenia patients (18 first episodes, FE), compared to 53 healthy controls. The EEG was acquired with subjects performing an odd-ball task. Analyses included an adaptive window of interest to take into account the interindividual variability of P300 latency. We compared source activation patters to distractor (P3a) and target (P3b) tones within- and between-groups.

Results: Patients showed a reduced activation in anterior cingulate and lateral and medial prefrontal cortices, as well as inferior/orbital frontal regions. This was also found in the FE patients alone. The activation was directly related to IQ in the patients and controls and to working memory performance in controls. Symptoms were unrelated to source activation. Fractional anisotropy in the tracts connecting lateral prefrontal and anterior cingulate regions predicted source activation in these regions in the patients.

Conclusions: These results replicate the source activation deficit found in a previous study with smaller sample size and a lower number of sensors and suggest an association between structural connectivity deficits and functional alterations.

Key words: schizophrenia, LORETA, EEG, diffusion tensor, anterior cingulate**.**

INTRODUCTION

Underpinnings of cognitive alterations in schizophrenia can be assessed with high temporal resolution using electroencephalographic (EEG) techniques, which are however limited by their spatial resolution. This problem can be partially overcome with source imaging approaches to detect EEG neural generators such as low-resolution brain electromagnetic tomography (LORETA) that allow for an acceptable compromise between spatial and temporal resolutions. LORETA is a reliable inverse problem method associated with low error rates [12, 23]. Therefore, it can provide relevant information about the cerebral dysfunction in schizophrenia.

One of the most usual paradigms for assessing neural dysfunction in schizophrenia is the auditory odd-ball task. The 3-stimulus variant of the auditory-oddball paradigm includes infrequent-distractor stimuli interspersed randomly into a sequence of frequent-standard and rare-target tones. The resulting P300 waveform includes P3a and the P3b components, elicited by distractor and target stimuli, respectively. Several studies using LORETA have been performed to describe EEG source patterns of these components in schizophrenia during auditory odd-ball tasks, whose partially discrepant results can be summarized as follows. An hypoactivation was found in patients in prefrontal, posterior cingulate and temporal cortex [37]. Using current source density analyses an asymmetrical reduction was described over the left insula, superior temporal gyrus (STG) and post-central gyrus in neuroleptic-naïve patients [35] as well as in left STG, middle frontal gyrus, precuneus and precentral lobe in 16 chronic schizophrenia patients [11]. Likewise, using the combination of LORETA and magnetic resonance imaging (MRI), reduced current density was found in left medial temporal and inferior parietal, with an hyperactive frontal lobe [22]. Finally, hypoactivation in the cingulate area during an auditory 2-tone oddball was found in 20 schizophrenia patients [29].

Those studies usually assessed neural sources with a large fixed post-stimulus window of interest (WOI) [11, 22, 33-35, 38]. This issue can hamper the results given the large inter-subject variability of P300 latency [6]. In order to overcome this problem we recently reported an analysis of neural sources during a P300 paradigm using an adaptive WOI, i.e., analyzing the ERP activity according to the actual latency in each subject. Hence, using a 29-electrodes array, we described significantly smaller P3b source current density for Sz patients in superior, middle and medial frontal, and cingulate gyrus [2].

In order to describe the alterations in P300 generators in schizophrenia is necessary to consider the generation of this ERP activity by a wide neural network [4, 31], with nodes likely connected by white matter tracts. Considering the relevance of structural connectivity alterations in schizophrenia [25, 36], the understanding of functional

deficits identified using LORETA may benefit from complementary information provided by diffusion magnetic resonance (dMR) gathered in the same patients.

Therefore, and considering the discrepancies among previous studies, the main aim of this study is to replicate the findings of our previous report [2] in an entirely new sample, using an adaptive WOI and a denser array of EEG electrodes, and including a larger proportion of first episodes (FE). This study would be of interest given the usually low rate of replication of biological findings in schizophrenia research. Additionally, we explored the association of differences in source density patterns with structural connectivity data (using dMR) and cognitive performance to achieve a better understanding of the possible substrates and relevance of functional alterations.

SUBJECTS AND METHODS

EEG data was acquired in 53 healthy controls and 38 schizophrenia patients (21 stable chronic and 17 FE patients) were recruited for the present study. Of them, dMR data were available for 16 healthy controls and 27 patients. None of these subjects was included in our previous LORETA study. Diagnoses were made by one experienced psychiatrist (VM) using the criteria from the Diagnostic and Statistical Manual of Mental Disorders, 5th edition. Chronic patients received stable doses of atypical antipsychotics, 14 of them in monotherapy (7 received also serotonin reuptake inhibitors and 5 benzodiazepines). FE patients were also receiving stable doses of antipsychotics, most of them having received this treatment for less than 15 days, with a wash-out period of 24 hours prior to EEG acquisition. This way, we expected the effects of treatment on the EEG be minimized in the FE group without affecting the clinical state of the patients. In both groups, antipsychotic doses were converted to chlorpromazine equivalents (table 1). Positive, negative and total symptoms were scored using the Positive and Negative Syndrome Scale (PANSS) [14].

Exclusion criteria for patients and controls were: (i) any neurological illness; (ii) history of cranial trauma with loss of consciousness longer than one minute; (iii) past or present substance abuse, except nicotine or caffeine (iv) total intelligence quotient (IQ) smaller than 70; and (v) for patients, presence of any other psychiatric process, and (vi) for controls, any current psychiatric or neurological diagnosis or treatment.

Healthy controls were recruited through newspaper advertisements.

Demographic and clinical characteristics are shown in Table 1.

Cognitive data from patients and controls were collected using the Wechsler Adult Intelligence Scale WAIS-III (IQ), the Spanish version of the Brief Assessment in Cognition in Schizophrenia Scale (BACS) [30] and the Wisconsin Card Sorting Test (percent of perseverative errors and number of completed categories). Seven patients did not

complete the cognitive assessment, and their cognitive data were not used in the analyses.

All participants gave their written informed consent after receiving full printed information. The ethical committees of the participating hospitals approved the study.

Electroencephalographic recordings

EEG data were acquired using a 33-channel EEG system (BrainVision®, Brain Products GmbH). Active electrodes were placed in an elastic cap at Fp1, Fp2, F7, F3, Fz, F4, F8, FC5, FC1, FCz, FC2, FC6, T7, C3, Cz, C4, T8, TP9, CP5, CP1, CP2, CP6, TP10, P7, P3, Pz, P4, P8, PO9, PO10, O1, Oz, O2 (international 10–10 system; impedance kept under 5 kΩ). Thirteen minutes of eyes-closed EEG activity were obtained during an auditory odd-ball 3-stimulus paradigm, which consisted of 600 random sequences of target (500 Hz-tone, probability 0.2), distractor (1000 Hz-tone, probability 0.2), and standard (2000 Hz-tone, probability 0.6) tones. Participants were instructed to press a button when detecting the target tones. Target tones were considered 'attended' tones whether they were followed by a button press. Only 'attended' target tones were considered for subsequent P3b analyses [10]. Moreover, distractor tones were considered for P3a analyses.

A sampling frequency of 500 Hz was used to acquire EEG activity. EEG recording were initially referenced over Cz electrode and subsequently re-referenced to the average activity of all sensors [4]. Preprocessing of EEG activity included several steps. Initially, a finite impulse response (FIR) band-pass filter (1–70 Hz, Hamming window) and a notch filter to remove the power line frequency interference (50 Hz, Butterworth filter) were applied to EEG data. In a second step, a three-step approach was used to remove artifacts [1, 10]: (i) each EEG recording was decomposed using independent component analysis (ICA) into a total of 33 components to detect and discard ICA components related to eye-blinks and muscle artifacts, after a visual inspection of their scalp maps and temporal activation; (ii) continuous ERP data were segmented into trials of 1 s, ranging from -300 ms before target stimulus onset to 700 ms after onset; and (iii) trials contaminated with artifacts were automatically detected and rejected in case their amplitude exceeded a statistical-based local adaptive threshold [1]. Finally, 1s-length artifact-free ERP trials were averaged for each channel and subject to obtain the evoked response, i.e., phase-locked to the stimulus onset [2]. Fig. 1 depicts the time evolution of P3a and P3b averaged evoked response for each group.

sLORETA neural generator analysis

Standardized LORETA (sLORETA) software assesses a particular solution of the non-unique EEG inverse problem [23]. It estimates the source current density in a brain model represented by a total of 6239 cubic voxels with 5 mm resolution [23]. Particularly, sLORETA is based on a realistic head model from Montreal Neurological

Institute (MNI) [18], in which the 3-D solution space was restricted to only the cortical gray matter [16].

LORETA source imaging studies commonly used a large fixed post-stimulus WOI, such as [250 500] ms. However, in this study we took into account P300 latency changes across subjects. P3a and P3b source images for each participant were averaged using the time window defined by a subject-adaptive WOI [2].

Diffusion MRI acquisition and processing

Magnetic resonance data were acquired with a Philips Achieva 3T unit. Both T1-weighted and diffusion weighted images were obtained. Acquisition parameters included: turbo field echo sequence for the T1, with 1 x 1 x 1 mm^3 of spatial resolution, 256 x 256 matrix size and 160 sagittal slices. For the diffusion data, b-value was set to 1000 s/mm^2. 61 gradient directions were employed, with 2 x 2 x 2 mm^3 of spatial resolution, 128 x 128 matrix size and 66 axial slices.

 The anatomical (T1) and the diffusion weighted images were afterwards processed following the procedure detailed in (Molina et al., 2017) in order to obtain connectivity matrices describing the connections each pair of cortical regions by means of the mean fractional anisotropy along the streamlines connecting them. Using Freesurfer (http://surfer.nmr.mgh.harvard.edu), FSL (http://fsl.fmrib.ox.ac.uk) MRtrix (www.mrtrix.org), 84x84 connectivity matrices were calculated. A (simplified) diagram of the processing pipeline is depicted in Fig. 2.

Statistics

Sociodemographic and cognitive data were compared between patients and controls using t tests and Chi-square tests when appropriate.

Firstly, we compared the P3a and P3b source generator patterns within each group (patients and controls) separately. Statistical differences were computed at each voxel by using paired-sample *t*-tests over log-transformed sLORETA images. Then, the corresponding between-groups comparisons of source activation for both P3a and P3b were carried out using voxel-by-voxel independent *t*-tests. In both statistical analyses, a correction for multiple comparisons were performed by means of a voxel intensity nonparamentric permutation test (NPT). It calculates a critical *t*-value by means of a random sample of all the possible permutations [21]

In a second step, we tested the hypothesis that EEG activation differences would contribute significantly to cognitive performance and symptoms. To this end multivariate stepwise regression analyses were used: averaged current density in Brodmann areas (BA) with statistically significant differences between groups were

included as independent variables and cognition or symptoms scores are the dependent ones. We carried out two previous steps to ensure the regression requirements were met. First, current density values were normalized using log-transformation. Second, we assessed collinearity among data by calculating the correlation coefficients between density values in those BA. These coefficients were high ($0.81 < r < 0.96$). Therefore, a principal components analysis (PCA), which extracted factors summarizing density, was performed to avoid colineariy effects on regression. We saved individual factor scores and used them in regression analyses.

To test whether structural connective deficits could predict functional abnormalities, we applied a new regression model: independent variables were the FA values in the tracts connecting the major regions showing between-groups deficits in source density, and dependent variables were the mean density values in these regions (as the factor scores calculated in the previous step).

Finally, we assessed the relation between the current treatment dose and source activation in the areas with significant between-group differences using correlation coefficients.

RESULTS

Age and sex distribution did not differ significantly between patients and controls. Patients showed a generalized cognitive deficit in comparison to controls (table 1). According to clinical interviews, no patient or control subject had a history of loss of consciousness in the past as a consequence of trauma.

Source density analyses

First of all, the neural sources associated with P3a and P3b were estimated for each group. As Fig. 3a shows, in the control group, within-group comparison showed a greater source current density for P3b as compared to P3a bilaterally in medial frontal and anterior cingulate, inferior frontal, posterior cingulate and superior parietal. In patients, source current density was larger for P3b in medial and inferior occipital. This was also found in the FE analyzed alone.

Between-groups comparisons for P3b are depicted in Fig. 3b. We found smaller source current density for patients in the lateral and medial frontal, anterior cingulate and inferior/orbital frontal regions, also found in the FE group. The corresponding BA are shown in Table 2.

We found no significant between groups source differences for P3a.

Source activation, cognition and symptoms

In order to summarize the source activation differences between patients and controls, we performed a PCA. This analysis on mean density yielded only a single factor, explaining 95.26% of variance (eigenvalue 7.63).

Factor scores of this analysis significantly explained total IQ in the patients (R^2=0.152, df=1,28, F=5.17, $β$=0.40, p=0.02) and the control (R^2=0.116, df =1,47, F=6.14, $β$=0.34, p=0.017) groups (Fig. 4a). There were no associations with individual BACS scores in the patients: 0.002 (motor speed)<R^2<0.093 (working memory). In the controls, LORETA density factor scores positively predicted working memory (R^2=0.164, df =1, 47, F=9.20, $β$=0.40, p=0.004).

Positive (r=-0.32, p=n.s) and negative (r=0.026) symptoms were not predicted by LORETA density scores.

Source activation and structural connectivity

Next, we aimed to explore the possible relations between structural connectivity and source density alterations.

The areas showing significant differences in source density between patients and controls were located on lateral frontal and anterior cingulate areas. Therefore, we tested the possible relationship between FA in the connections linking anterior cingulate and middle frontal prefrontal area.

Fractional anisotropy in the tract linking middle prefrontal with anterior cingulate was found predictive of EEG activation (R^2=0.198, df=1.25, F=6.16, $β$=0.44, p=0.02) (Fig 4b), but not in controls (R^2=0.013, p=n.s.).

Relation with treatment

Doses were inversely associated to factor scores summarizing activation in the regions with between-group differences (r=-0.44, p=0.016) (Fig. 5). In particular, this association was statistically significant for BA10 (r=-0.54, p=0.005), BA11 (r=-0.48, p=0.01), BA9 (r=-0.56, p=0.003), BA47 (r=-0.51, p=0.008), and BA25 (r=-0.49, p=0.01).

There was no association between illness duration and factor scores summarizing activation in the regions with between-groups differences (r=0.009, p=ns).

DISCUSSION

Our control subjects showed larger source differences for P3b than patients in parietal and frontal regions. In the direct comparison between patients and controls, P3b source activation was smaller in Sz patients over medial frontal and anterior cingulate gyrus (BA9, BA32, BA33), lateral prefrontal (BA9, 10 and 11) and orbital frontal gyrus (BA11, BA25). These results essentially replicate those of our former study by using a novel and large database [2]. Patients also showed larger medial and inferior occipital source

activation for P3b as compared to P3a. However, the relevance of that data seems questionable, since no between-group differences were found at this level.

However, our findings did not depict differences in P3a sources between groups, supporting that different activation in patients relates to relevance rather than to novelty. P3a may be generated whether sufficient attentional focus is engaged. In contrast, P3b seems to be related to conscious top-down target processing, likely contributing to processing the stimulus information and performing cognitive response [26, 32].

Using functional magnetic resonance imaging (fMRI), previous studies localized the sources of auditory P3b in a distributed network that includes superior and medial temporal, posterior parietal, hippocampal, cingulate and frontal structures [26, 32, 34, 38]. Previous studies using LORETA also support a role for cingulate and frontal areas[34] and in the posterior cingulate[38] in P3b generation. Earlier studies also identified the P3 sources in anterior cingulate region using Brain Electrical Source Analysis [7]. Therefore, according to our results, schizophrenia patients showed a reduced activation in the network expected to participate in P3b generation. [35].

In agreement with previous studies focused on schizophrenia, our patients showed smaller P3b activity source in bilateral anterior medial cortex, including the medial frontal and cingulate areas [15, 29, 37]. Likewise, a P3b current density reduction was reported in non-deficit Sz patients during a 3-tone oddball paradigm in bilateral frontal and cingulate areas [20]. Intriguingly, in that study [20] deficit schizophrenia patients did not show P3b source reduction. Other coherent results have been reported with other imaging techniques, such as the reductions in medial frontal and anterior cingulate [5] and cingulate [3] volumes in schizophrenia.

Structural connectivity deficits between these areas could contribute to an alteration in activation patterns in this network. This is suggested by the relation between reduced source activation and FA values(reflecting white mater integrity) in the middle-prefrontal to cingulate white matter tract. Interestingly, FA was significantly reduced in this tract in schizophrenia patients in comparison to controls [19]. Therefore, structural connectivity deficits could have a negative influence on the capacity for coordinating the activation of cingulate and prefrontal areas, which, in turn, may hamper cognitive performance according to its association to total IQ. In controls, activation in the areas with significant between-groups differences positively related to working memory, which is coherent with the involvement of prefrontal regions in this function[9].

In FE patients, we also observed an activation deficit in superior and medial frontal cortices, suggesting that such deficit is not simply secondary to chronicity and previous treatment. However, there was a significant inverse relation between source activation and antipsychotic dose, supporting a role for current treatment in activation deficit in patients. Taken together, the findings of the present study suggest that regions involved

in P3b task are hypoactive in schizophrenia in relation to structural connectivity, although that hypoactivation can be aggravated by antipsychotics.

The P3b potential has been proposed to reflect context updating [8], i.e., the process by which changes in internal and external information are detected and used to guide behavior according to current demands. Recent interpretations of this process distinguish three components: (i) detection of changes in context; (ii) activation of representation of the new context; and (iii) reconfiguration of the mechanisms responsible of performing the new task [17]. The prefrontal cortex plays an active role in maintaining context representations in working memory [24], and therefore is a key element in context updating. In this framework, it has been proposed that the posterior positivity that usually characterized P3b may reflect the reconfiguration process in posterior pathways following context updating, largely in the PFC [17]. Using a modified CPT design to examine effects of context updating, a previous study [17] identified the earliest effects at 200 ms with a topography consistent with a prefrontal generator, followed at 400-700 ms by an activation over posterior areas and finally an effect whose generator was likely in the medial frontal region. Our patients did not show the PFC and medial PF activations during a task requiring assessment of the context (the preceding tone) to issue an adequate response. This can suggest a decreased capacity for updating context in the patients that can be reflected in their reduced cognitive performance associated with their reduced cortical activation during P3b.

Our patients were performing an odd-ball task. Therefore, the source activation differences observed in comparison to controls would not necessarily be found under other conditions. However, we find interesting that some of the hypoactive areas (medial prefrontal and cingulate) may have a key role in the subjective experience of the self [27], considering that self-experience deficits are proposed to be central in schizophrenia [28].

Other studies revealed decreased current densities in other areas during P300 task in schizophrenia, such as temporal cortex in 18 patients[37], insula, STG and post-central gyrus in 19 patients [35] and left medial temporal and inferior parietal in 20 patients [22]. Total BPRS scores negatively correlated with current density at left STG and right medial prefrontal [13]. Since the degree of replication is lower for findings in these areas than in cingulate or frontal lobes, differences in methodologies and small sample size might have played a role.

Our study has limitations, notably in relation to the role of treatment in source activation deficits. In relation to this issue, although we could have minimized its effects with a 24 h wash-out in FE patients, treatment effects may last for a longer period. Although it would be necessary to replicate our findings in a completely neuroleptic-naïve sample, we conclude that a deficit of activation of the fronto-cingulate network during a cognitive task may play a relevant role in the pathophysiology of schizophrenia.

Moreover, it could be of interest to assess differences between clinical subtypes of schizophrenia, which might help to elucidate phenotypes within this syndrome.

ACKNOWLEDGEMENTS

Conflict of interest.

None of the authors have any conflict of interest to declare.

REFERENCES

1. Bachiller A, Poza J, Gomez C, Molina V, Suazo V, Hornero R (2015) A comparative study of event-related coupling patterns during an auditory oddball task in schizophrenia. J Neural Eng 12:016007

2. Bachiller A, Romero S, Molina V, Alonso JF, Mananas MA, Poza J, Hornero R (2015) Auditory p3a and p3b neural generators in schizophrenia: An adaptive sloreta p300 localization approach. Schizophr Res 169:318-325

3. Baiano M, David A, Versace A, Churchill R, Balestrieri M, Brambilla P (2007) Anterior cingulate volumes in schizophrenia: A systematic review and a meta-analysis of mri studies. Schizophr Res 93:1-12

4. Bledowski C, Prvulovic D, Hoechstetter K, Scherg M, Wibral M, Goebel R, Linden DE (2004) Localizing p300 generators in visual target and distractor processing: A combined event-related potential and functional magnetic resonance imaging study. J Neurosci 24:9353-9360

5. Bora E, Fornito A, Radua J, Walterfang M, Seal M, Wood SJ, Yucel M, Velakoulis D, Pantelis C (2011) Neuroanatomical abnormalities in schizophrenia: A multimodal voxelwise meta-analysis and meta-regression analysis. Schizophr Res 127:46-57

6. Campanella S, Gomez C, Rossion B, Liard L, Debatisse D, Dubois S, Delinte A, Bruyer R, Crommelinck M, Guerit JM (1999) [a comparison between group-average and individual evoked potential analysis]. Neurophysiol Clin 29:325-338

7. Dien J, Spencer KM, Donchin E (2003) Localization of the event-related potential novelty response as defined by principal components analysis. Brain Res Cogn Brain Res 17:637-650

8. Donchin E, Coles M (1988) P300 component, a manifestation of cognitive updating? Behav Brain Sci 11:357-427

9. Goldman Rakic PS (1994) Working memory dysfunction in schizophrenia. J Neuropsychiatry Clin Neurosci 6:348-357

10. Gómez-Pilar J, Poza J, Bachiller A, Gómez C, Molina V, Hornero R (2015) Neural network reorganization analysis during an auditory oddball task in schizophrenia using wavelet entropy. . Entropy 17:5241-5256

11. Higuchi Y, Sumiyoshi T, Kawasaki Y, Matsui M, Arai H, Kurachi M (2008) Electrophysiological basis for the ability of olanzapine to improve verbal memory and functional outcome in patients with schizophrenia: A loreta analysis of p300. Schizophr Res 101:320-330

12. Jung HT, Kim DW, Kim S, Im CH, Lee SH (2012) Reduced source activity of event-related potentials for affective facial pictures in schizophrenia patients. Schizophr Res 136:150-159

13. Kawasaki Y, Sumiyoshi T, Higuchi Y, Ito T, Takeuchi M, Kurachi M (2007) Voxel-based analysis of p300 electrophysiological topography associated with positive and negative symptoms of schizophrenia. Schizophr Res 94:164-171

14. Kay SR, Fiszbein A, Opler LA (1987) The positive and negative syndrome scale (panss) for schizophrenia. Schizophr Bull 13:261-276

15. Kim DW, Shim M, Kim JI, Im CH, Lee SH (2014) Source activation of p300 correlates with negative symptom severity in patients with schizophrenia. Brain Topogr 27:307-317

16. Lancaster JL, Woldorff MG, Parsons LM, Liotti M, Freitas CS, Rainey L, Kochunov PV, Nickerson D, Mikiten SA, Fox PT (2000) Automated talairach atlas labels for functional brain mapping. Hum Brain Mapp 10:120-131

17. Lenartowicz A, Escobedo-Quiroz R, Cohen JD (2010) Updating of context in working memory: An event-related potential study. Cogn Affect Behav Neurosci 10:298-315

18. Mazziotta J, Toga A, Evans A, Fox P, Lancaster J, Zilles K, Woods R, Paus T, Simpson G, Pike B, Holmes C, Collins L, Thompson P, MacDonald D, Iacoboni M, Schormann T,

Amunts K, Palomero-Gallagher N, Geyer S, Parsons L, Narr K, Kabani N, Le Goualher G, Boomsma D, Cannon T, Kawashima R, Mazoyer B (2001) A probabilistic atlas and reference system for the human brain: International consortium for brain mapping (icbm). Philos Trans R Soc Lond B Biol Sci 356:1293-1322

19. Molina V, Lubeiro A, Soto O, Rodriguez M, Alvarez A, Hernandez R, de Luis-Garcia R (2017) Alterations in prefrontal connectivity in schizophrenia assessed using diffusion magnetic resonance imaging. Prog Neuropsychopharmacol Biol Psychiatry 76:107-115

20. Mucci A, Galderisi S, Kirkpatrick B, Bucci P, Volpe U, Merlotti E, Centanaro F, Catapano F, Maj M (2007) Double dissociation of n1 and p3 abnormalities in deficit and nondeficit schizophrenia. Schizophr Res 92:252-261

21. Nichols TE, Holmes AP (2002) Nonparametric permutation tests for functional neuroimaging: A primer with examples. Hum Brain Mapp 15:1-25

22. Pae JS, Kwon JS, Youn T, Park HJ, Kim MS, Lee B, Park KS (2003) Loreta imaging of p300 in schizophrenia with individual mri and 128-channel eeg. Neuroimage 20:1552-1560.

23. Pascual-Marqui RD (2002) Standardized low-resolution brain electromagnetic tomography (sloreta): Technical details. Methods Find Exp Clin Pharmacol 24 Suppl D:5-12

24. Passingham D, Sakai K (2004) The prefrontal cortex and working memory: Physiology and brain imaging. Curr Opin Neurobiol 14:163-168

25. Pettersson-Yeo W, Allen P, Benetti S, McGuire P, Mechelli A (2011) Dysconnectivity in schizophrenia: Where are we now? Neurosci Biobehav Rev 35:1110-1124

26. Polich J (2007) Updating p300: An integrative theory of p3a and p3b. Clin Neurophysiol 118:2128-2148

27. Qin P, Northoff G (2011) How is our self related to midline regions and the default-mode network? Neuroimage 57:1221-1233

28. Saas LA, Parnas J (2007) Explaining schizophrenia: The relevance of phenomenology. In: Cheung Chung M, K.W.M. F, Graham G (eds) Reconceiving schizophrenia. Oxford Univ Press, New York, p 63-92

29. Sabeti M, Moradi E, Katebi S (2011) Analysis of neural sources of p300 event-related potential in normal and schizophrenic participants. Adv Exp Med Biol 696:589-597

30. Segarra N, Bernardo M, Gutierrez F, Justicia A, Fernadez-Egea E, Allas M, Safont G, Contreras F, Gascon J, Soler-Insa PA, Menchon JM, Junque C, Keefe RS (2011) Spanish validation of the brief assessment in cognition in schizophrenia (bacs) in patients with schizophrenia and healthy controls. Eur Psychiatry 26:69-73

31. Soltani M, Knight RT, Yamaguchi S, Chao LL, Nielsen-Bohlman L (2000) Neural origins of the p300. Crit Rev Neurobiol 14:199-224.

32. Strobel A, Debener S, Sorger B, Peters JC, Kranczioch C, Hoechstetter K, Engel AK, Brocke B, Goebel R (2008) Novelty and target processing during an auditory novelty oddball: A simultaneous event-related potential and functional magnetic resonance imaging study. Neuroimage 40:869-883

33. Sumiyoshi T, Higuchi Y, Kawasaki Y, Matsui M, Kato K, Yuuki H, Arai H, Kurachi M (2006) Electrical brain activity and response to olanzapine in schizophrenia: A study with loreta images of p300. Prog Neuropsychopharmacol Biol Psychiatry 30:1299-1303

34. Volpe U, Mucci A, Bucci P, Merlotti E, Galderisi S, Maj M (2007) The cortical generators of p3a and p3b: A loreta study. Brain Res Bull 73:220-230

35. Wang J, Tang Y, Li C, Mecklinger A, Xiao Z, Zhang M, Hirayasu Y, Hokama H, Li H (2010) Decreased p300 current source density in drug-naive first episode schizophrenics revealed by high density recording. Int J Psychophysiol 75:249-257

36. Wheeler AL, Voineskos AN (2014) A review of structural neuroimaging in schizophrenia: From connectivity to connectomics. Frontiers in human neuroscience 8:653

37. Winterer G, Mulert C, Mientus S, Gallinat J, Schlattmann P, Dorn H, Herrmann WM (2001) P300 and loreta: Comparison of normal subjects and schizophrenic patients. Brain Topogr 13:299-313.

38. Wronka E, Kaiser J, Coenen AM (2012) Neural generators of the auditory evoked potential components p3a and p3b. Acta Neurobiol Exp (Wars) 72:51-64

	Patients	FE patients	Controls
Age	32.77 (8.70)	29.33 (8.03)	31.43 (9.50)
Sex (Male:Female)	22:16	11:7	29:24
CPZ equivalents (mg/d)	396.80 (205.67)	357.14 (215.82)	
Duration(months)	74.19 (110.21)	25.14 (62.75)	
Study years	14.20 (3.71)	14.88 (3.42)	
Positive symptoms	11.58 (3.46)	12.92 (4.42)	
Negative symptoms	17.19 (6.94)	10.35 (2.06)	
Total symptoms	54.01 (19.02)	44.80 (8.73)	
Total intelligence quotient (WAIS)	92.34 (15.58) ***	87.35 (13.33) ***	109.46 (12.166)
Verbal memory (BACS)	35.70 (12.52)**	37.00 (12.30)***	51.62 (8.66)
Working memory (BACS)	17.19 (5.12) ***	17.12 (4.83)**	20.646 (4.03)
Motor speed (BACS)	60.14 (16.13) ***	57.70 (11.61) ***	72.041 (14.23)
Verbal fluency (BACS)	19. 71 (5.29) ***	17.62 (5.48) ***	27.77 (5.77)
Processing speed (BACS)	45.43 (15.03) ***	49.23 (12.16) ***	70.02 (14.24)
Problem solving (BACS)	15.94 (5.19) *	14.44 (5.56)*	17.12 (2.62)
WCST perseverative errors (%)	16.81 (11.09) ***	15.40 (8.48)**	9.88 (5.81)
WCST completed categories	4.82 (1.81) **	4.65 (1.83)***	5.75 (0.81)
Number of P3a artifact-free epochs	74.55 (16.23)	77.17 (18.30)	80.21 (10.71)
P3a amplitude at Pz (µV)	126.89 (99.35)*	131.27 (105.49)	181.97 (117.07)
Number of P3b artifact-free epochs	71.21 (16.04)	76.67 (12.93))	77.04 (13.20)
P3b amplitude at Pz (µV)	163.83 (112.85)***	173.69 (129.55)**	279.27 (174.60)

Table 1. Clinical and demographic data in patients and controls. Data are shown as mean (sd). CPZ: chlorpromazine; WAIS: Weschler Assessment of Intelligence Scale; WCST: Wisconsin card Sorting Test; BACS: Brief Assessment of Cognition in Schizophrenia (see text). Significance of between-group comparisons (Sz patients vs. controls and FE vs controls) are shown (*$p<0.05$; **$p<0.01$; ***$p<0.001$).

	Critical t-value	Lobe	Gyrus	Brodmann Area
Sz Patients *vs* **Controls**	2.597	Frontal (538 vox; 25%) **Limbic (184 vox; 24%)**	Medial frontal gyrus (207 vox; 58%) Superior frontal gyrus (148 vox; 38%) **Anterior cingulate (144 vox; 100%)** Inferior frontal gyrus (57 vox; 16%) Rectal gyrus (44 vox; 100%) Cingulategyrus (39 vox; 14%) Middle frontal gyrus (35 vox; 7%) Orbital gyrus (29 vox; 94%) Subcallosalgyrus (17 vox; 71%)	ba10 (160 vox; 59%) ba11 (160 vox; 67%) ba9 (120 vox; 45%) ba32 (108 vox; 70%) ba47 (56 vox; 26%) **ba24 (55 vox; 36%)** ba25 (44 vox; 98%) ba33 (6 vox; 100%)
Sz Chronic *vs* **Controls**	2.319	Frontal (311 vox; 14%) **Limbic (112 vox; 15%)**	Medial frontal gyrus (166 vox; 46%) **Anterior cingulate (110 vox; 76%)** Superior frontal gyrus (95 vox; 24%) Middle frontal gyrus (30 vox; 6%) Rectal gyrus (9 vox; 20%) Orbital gyrus (7 vox; 22%)	ba10 (123 vox; 45%) ba9 (111 vox; 41%) **ba32 (81 vox; 52%)** ba11 (52 vox; 22%) ba24 (23 vox; 15%) ba8 (21 vox; 12%) ba25 (9 vox; 20%) ba33 (3 vox; 50%)
Sz First Episode *vs* **Controls**	2.797	**Limbic (183 vox; 24%)** Frontal (153 vox; 7%) Temporal (66 vox; 6%) Sub-lobar (10 vox; 4%)	**Cingulate gyrus (74 vox; 26%)** Anterior cingulate (70 vox; 49%) Inferior frontal gyrus (67 vox; 18%) Superior frontal gyrus (53 vox; 13%) Medial frontal gyrus (28 vox; 8%) Uncus (26 vox; 41%) Rectal gyrus (23 vox; 52%) Orbital gyrus (11 vox; 35%)	**ba24 (81 vox; 53%)** ba47 (69 vox; 21%) ba38 (64 vox; 40%) ba11 (51 vox; 21%) ba25 (38 vox; 84%) ba32 (30 vox; 19%) ba34 (16 vox; 48%) ba23 (15 vox; 29%) ba33 (6 vox; 100%)

Table 2. Results of P3b between-group brain-source density analyses. Critical t-value (t_{crit}) was estimated for each comparison applying a statistical threshold ($p < 0.05$) to voxel intensity NPT. Lobe, gyrus and Brodmann areas (BA) are only displayed when they obtained statistically significant differences after multiple comparisons correction (voxel intensity NPT, $t < t_{crit}$). Bold names of lobes, gyrus and BA represent, respectively, the lobe, the gyrus and the BA that contain the maximum voxel statistical t-value.
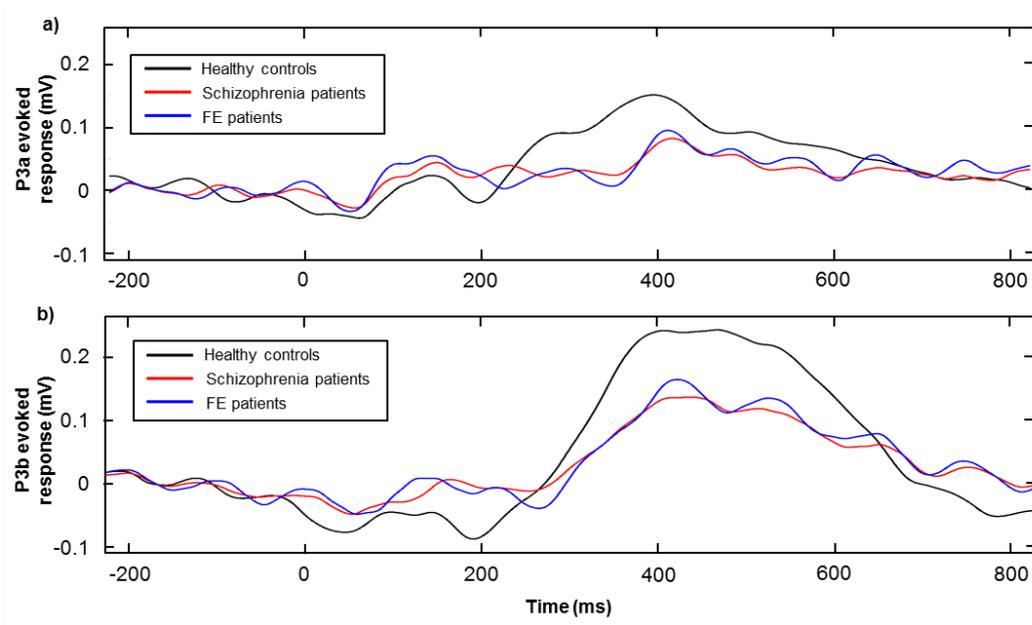
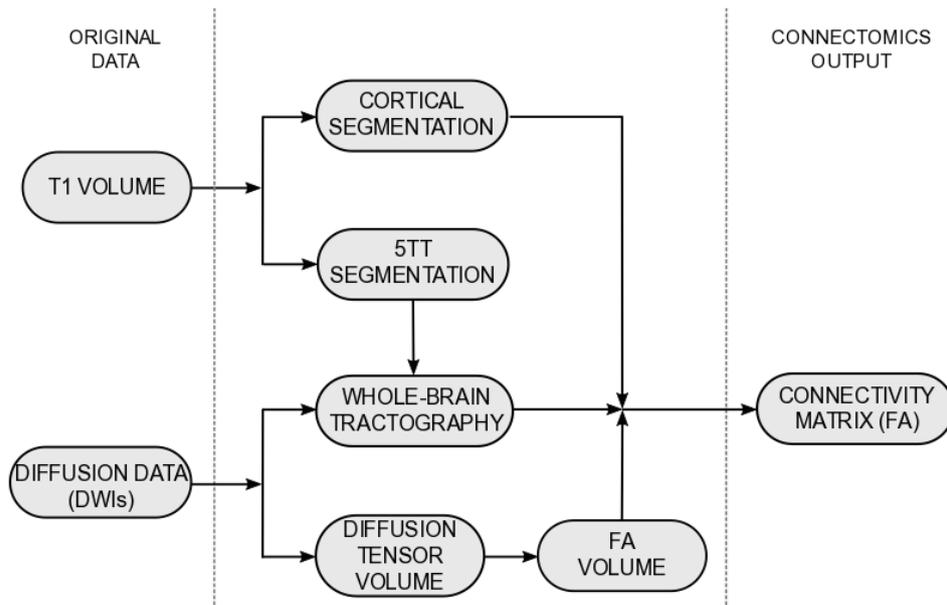**Figure 1.** Averaged evoked responses in each group for a) P3a tones; and b) P3b tones.

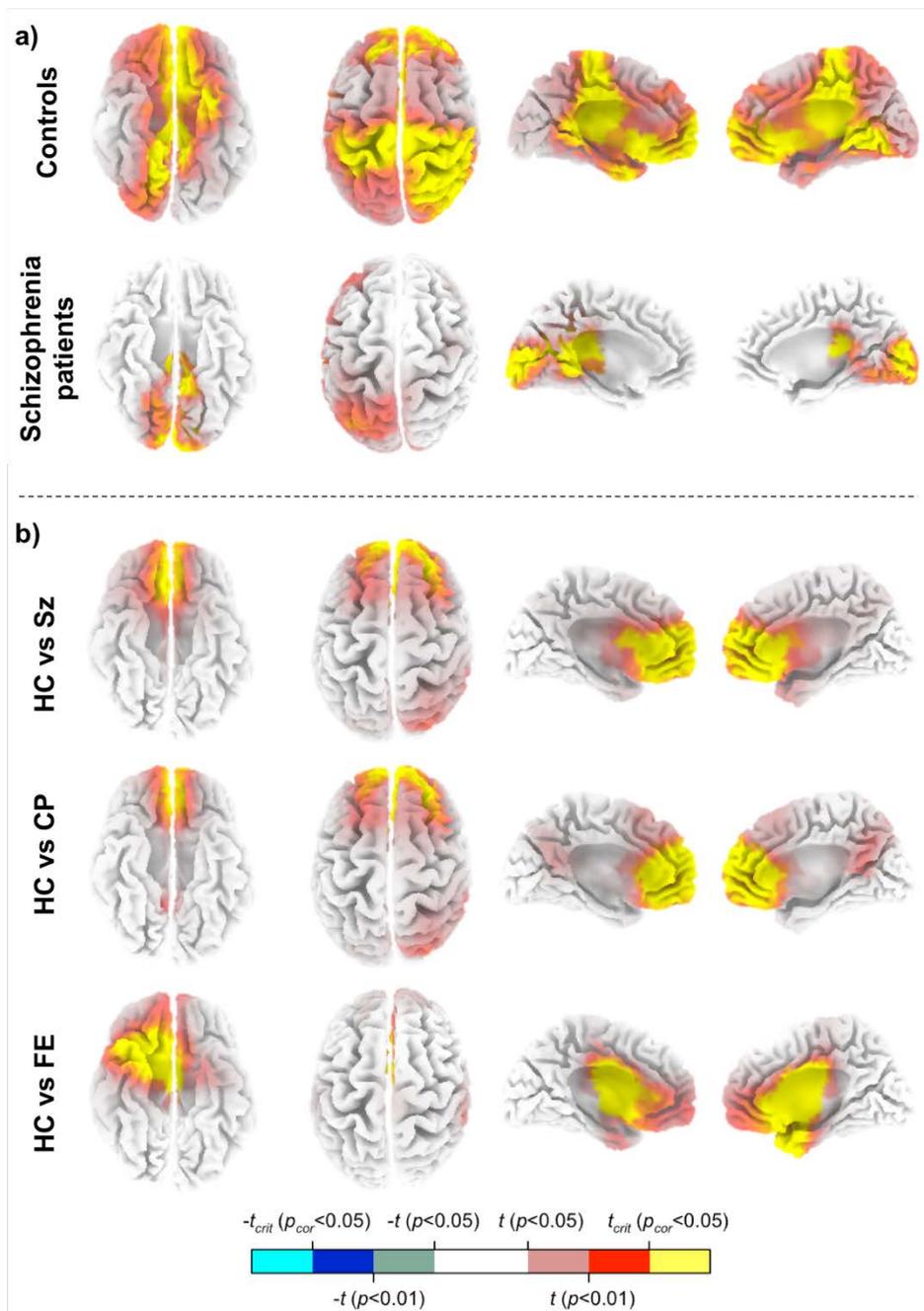**Figure 2.** Processing pipeline yielding fractional anisotropy values.

Figure 3. Three dimensional sLORETA maps of voxel-by-voxel statistical analysis. The scale shows negative (blue) and positive (yellow/red) t-values for which alpha is statistically significant after voxel intensity NPT correction for multiple comparisons. **a)** Paired sample *t*-statistics for healthy controls and schizophrenia patients. Cortical current density changes between P3b and P3a components are compared for each group. An increase of P3b source density from P3a is represented in yellow and vice versa. **b)** Differences in brain activation patterns between schizophrenia (Sz) patients and healthy controls (HC) using voxel-by-voxel independent *t*-statistics. Positive *t*-values represent larger source activity in control group than in Sz patients and vice versa.
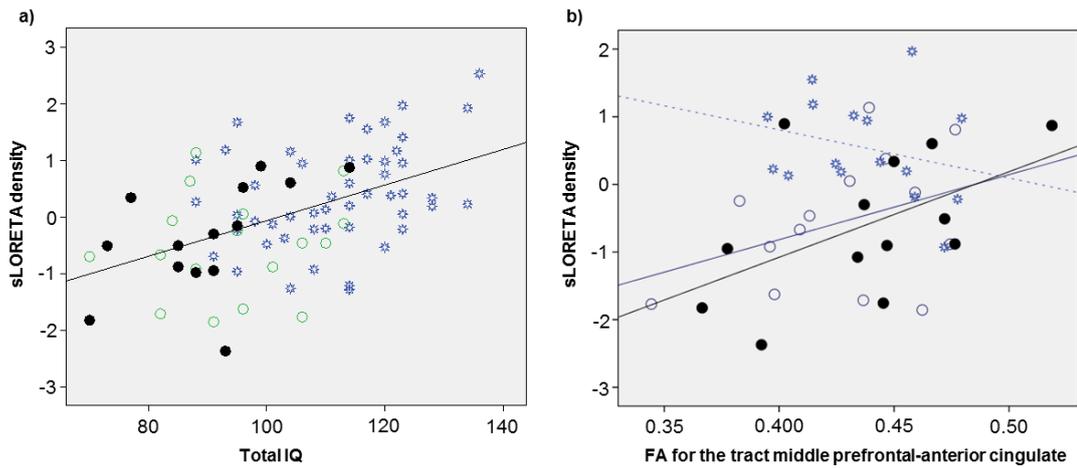
Figure 4. Significant associations with source activation. a) Scatterplot showing the association between factor scores summarizing mean density for the areas with significant between groups differences for P3b and total IQ scores, summarizing cognition for each subject. b) Scatterplot showing the association in the patients between FA in the White matter tract linking anterior cingulate and middle lateral prefrontal cortex. In this figure, the dotted regression line depicts the association in controls and the continuous lines depict the associations in FE and chronic patients. Stars: healthy controls, open dots chronic patients, solid dots FE patients.
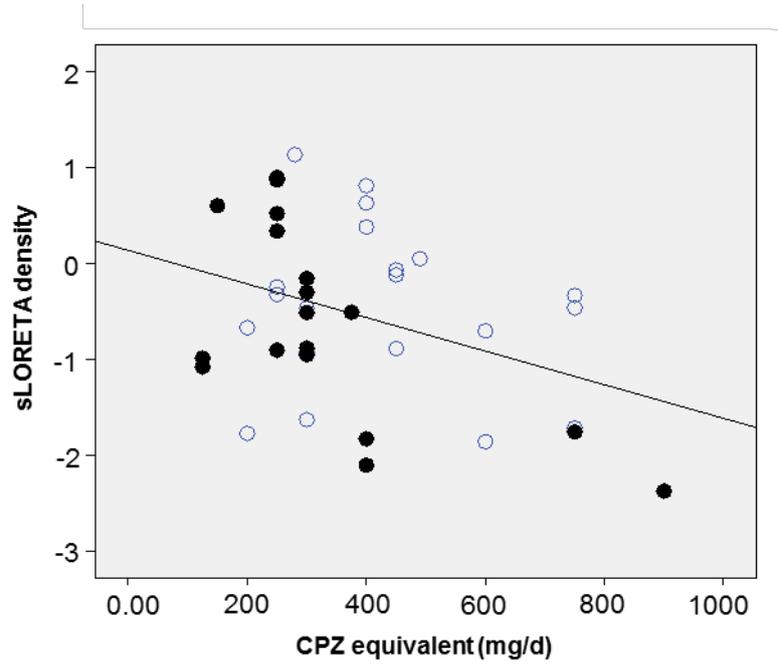
Figure 5. Scatterplot showing the association between treatment dose (in mg/d of chlorpromazine equivalents) and factor scores summarizing source activation in the regions with significant between-group differences in activation. Open dots represent chronic patients and solid dots FE patients.